We are IntechOpen,
the world's leading publisher of
Open Access books
Built by scientists, for scientists

4,800
Open access books available

122,000
International authors and editors

135M
Downloads

154
Countries delivered to

Our authors are among the

TOP 1%
most cited scientists

12.2%
Contributors from top 500 universities

WEB OF SCIENCE™

Selection of our books indexed in the Book Citation Index
in Web of Science™ Core Collection (BKCI)

Interested in publishing with us?
Contact book.department@intechopen.com

Fractal Light Vortices

Federico J. Machado, Juan A. Monsoriu and

Walter D. Furlan

Additional information is available at the end of the chapter

Abstract

Vortex lenses produce special wavefronts with zero-axial intensity, and helical phase structure. The variations of the phase and amplitude of the vortex produce a circular flow of energy that allows transmitting orbital angular momentum. This property is especially in optical trapping, because due to the orbital angular momentum of light, they have the ability to set the trapped particles into rotation. Vortex lenses engraved in diffractive optical elements have been proposed in the last few years. These lenses can be described mathematically as a two-dimensional (2D) function, which expressed in polar coordinates are the product of two different separable one-dimensional (1D) functions: One, depends only on the square of radial coordinate, and the other one depends linearly on the azimuthal coordinate and includes the topological charge. The 1D function that depends on the radial coordinate is known as a zone plate. Here, vortex lenses, constructed using different aperiodic zone plates, are reviewed. Their optical properties are studied numerically by computing the intensity distribution along the optical axis and the transverse diffraction patterns along the propagation direction. It is shown that these elements are able to create a chain of optical traps with a tunable separation, strength and transverse section.

Keywords: optical vortex, optical traps, diffractive optical elements (DOEs), fractal zone plates, devil's lenses, Thue-Morse sequence

1. Introduction

Vortex lenses (VLs) produce special wavefronts with zero-axial intensity, and helical structure with undefined phase in the vortex centre. These structures, called optical vortices [1–3], constitute an intriguing and growing area of research that combines fundamental theoretical aspects and novel applied technologies. A fundamental property of vortices is the conservation

INTECH
open science | open minds

of the topological charge which is defined as the 2π module of the total change of the phase along a closed curve surrounding the vortex centre. The variations of the phase and amplitude of the vortex produce a circular flow of energy that allows to carry orbital angular momentum [4, 5]. This property is useful for several applications, such as in astrophysics [6, 7], transmission of information [8, 9], microscopy [10], laser engraving [11] and especially in optical traps [12–16], because due to the orbital angular momentum of light, they have the ability to set the trapped particles into rotation.

Several methods have been proposed to obtain optical vortices [3, 4, 17–20] being spiral phase plates (i.e. lenses with a linear phase dependence on the azimuthal angle) and diffractive optical elements (DOEs) probably the most frequent approach. In fact, due to its simplicity, they can be employed in multiple applications. In particular, zone plates (ZPs) have found a great number of new applications in the last few years [21]. A standard amplitude ZP consists of a series of concentric circular rings of equal area, with alternating transmitting and absorbing zones. This means that along the square of the radial coordinate, a ZP can be thought as a periodic structure. The focusing effect is created by the constructive interference of waves passing through this structure.

On the other hand, in recent years different non-periodic and quasi-periodic sequences [22] have been also employed to design new types of ZPs with curious physical properties. Fractal zone plates (FrZPs) [23, 24], Fibonacci zone plates (FiZPs) [25, 26], Thue-Morse zone plates (TMZPs) [27] and some variations of these basic designs are representative examples [28–30].

FrZPs are characterized by its fractal structure along the square of the radial coordinate that produce multiple foci along the optical axis which are defined by the self-similar Fourier spectrum of the fractal pupil function [23]. These lenses produce a main focus surrounded by numerous secondary foci, which together result in a compound focal volume. It has been demonstrated that these self-similar foci produce reduction of the chromatic aberration under wideband illumination and increase of depth of field [24].

FiZPs are bifocal ZPs with their foci located at certain axial positions given by the Fibonacci numbers, being the 'golden mean', the ratio of the two focal distances [25]. As the name indicates, these lenses are designed following an aperiodic structure generated by the Fibonacci sequence. The focusing and imaging capabilities of Fibonacci lenses have been experimentally demonstrated under monochromatic illumination [26]; however, these lenses are affected by the same limitations of conventional ZPs when broadband illumination is considered, since the twin foci are not self-similar.

TMZPs are based on the deterministic Thue-Morse sequence, which results in a combination of the FrZP and FiZP. For this reason, this new family of aperiodic ZPs combines the advantages of fractal ZPs (reduction of the chromatic aberration) and Fibonacci ZPs (bifocusing along the optical axis) [27].

In this chapter, the combination of a vortex lens and ZPs, constructed using different aperiodic sequences, in a single element is considered. Their optical properties are investigated numerically and experimentally. The focusing properties of different combinations of FZPs and vortex lenses are studied by computing the intensity distribution along the optical axis and the

transverse diffraction patterns along the propagation direction. The diffracted field of these vortex lenses was obtained numerically within the Fresnel approximation.

We emphasize that these elements are able to create a chain of optical traps along the optical axis with a tunable separation, strength and transverse section. We discuss the influence of the topological charge on the irradiance propagation and also we investigate the variation of the angular momentum provided by the doughnut-shaped foci.

An optical set-up was implemented to obtain experimental results in which the VLs were registered in a spatial light modulator (SLM).

We have shown that our VLs are able to generate multiple-plane optical trappings with a volumetric extension. In this sense, they are superior to conventional vortices, whose extension is limited to the depth of focus of the beam.

2. Basic theory

The transmittance of a VL can be expressed as the product of two factors being the first one associated to a given ZP, which has only a radial dependence, and the other one corresponding to a vortex lens with a linear phase dependence on the azimuthal angle θ.

A ZP can be realized from a one-dimensional (1D) compact-supported periodic function $q(\zeta)$ as shown in **Figure 1**, where $\zeta = \left(\frac{r}{a}\right)^2$ is the normalized square radial coordinate and a is the external radius of the outermost ring. Therefore, in a binary ZP, every pair of opaque and transparent zones conforms a period. The area of each period is constant over all the ZPs.

In a similar way, the aperiodic zone plates that we consider from now on can be constructed by replacing the periodic function $q(\zeta)$ by either the Cantor function, the Fibonacci sequence or the Thue-Morse sequence. In fact, when designing VL, each of these sequences can be used to
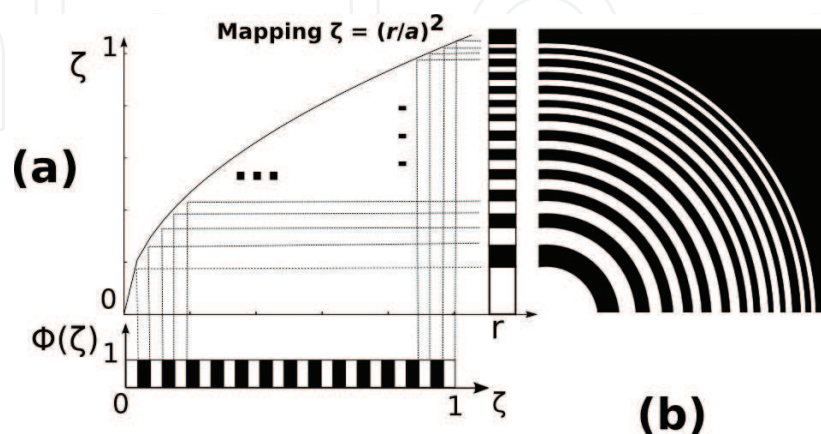

Figure 1. Schematic representation of the geometrical construction of a ZP from a periodic binary function. (a) Variable ζ mapped as function of r^2. (b) Layout of zones on ZP lens.

define the transmission generating function $q(\zeta)$ with compact support on the interval $\zeta \in [0, 1]$. This interval is partitioned in $2S$ sub-intervals of length $dS = \frac{1}{2S}$, and the transmittance value $t_{S,j}$, which takes at the jth sub-interval, is associated to the value of the element $D_{S,j}$, being $t_{S,j} = 1$ for the transparent zones and $t_{S,j} = 0$ for the opaque zones.

To study the focusing properties of VLs, we compute the irradiance provided by the transmittance of each lens described in general terms as

$$t(\zeta, \theta_0) = q(\zeta)\exp[im\theta_0], \tag{1}$$

where the azimuthal dependence is characterized by the topological charge m

We consider monochromatic plane wave illumination of wavelength λ. Thus, within the Fresnel approximation the irradiance function is given by

$$I(u, v; \theta) = u^2 \left| \int_0^1 \int_0^{2\pi} t(\zeta, \theta_0)\exp(-i2\pi u\zeta)\exp[i4\pi uv\zeta^{1/2}\cos(\theta - \theta_0)]d\zeta d\theta_0 \right|^2 \tag{2}$$

where $u = \frac{a^2}{2\lambda z}$ is the dimensionless reduced axial coordinate and $v = \frac{r}{a}$ is the normalized transverse coordinate [23]. By using Eq. (1) and taking into account that

$$\int_0^{2\pi} t(\zeta, \theta_0) \exp(-i2\pi u\zeta) \exp[i4\pi uv\zeta^{1/2}\cos(\theta - \theta_0)]d\theta_0 = 2\pi\exp\left[im\left(\theta + \frac{\pi}{2}\right)\right]J_m(4\pi uv\zeta^{1/2}) \tag{3}$$

Equation 2 is reduced to

$$I(u, v) = 4\pi^2 u^2 \left| \int_0^1 q(\zeta, \theta_0)\exp(-i2\pi u\zeta)J_m(i4\pi uv\zeta^{1/2})d\zeta \right|^2 \tag{4}$$

$J_m()$ being the Bessel function of the first kind of order m.

3. Fractal vortex lenses

Two different results were independently obtained by combining spiral phase plates with FrZP to produce a sequence of focused optical vortices along the propagation direction. In Ref. [31], the spiral fractal zone plate is generated as a phase-only FrZP modulated by helical phase structure. Another design of spiral phase plate based on a *blazed* FrZP, the devil's lens [32], was proposed to improve diffraction efficiency of a spiral FrZP. A devil's lens has a characteristic surface relief along the radial coordinate which is obtained using the devil's staircase function

[33]. It is because of its blazed profile that devil vortex lens has improved diffraction efficiency with respect to the spiral fractal zone.

The focal volume generated by Fresnel vortex lenses (FrVLs) results in a chain of vortices that could be used as versatile and very efficient optical tweezers because, in addition to rotating the trapped particles with high refractive index, other particles with a lower refractive index can be trapped in the vortex centre. The relative angular velocity of the particles at the different traps can be changed with different topological charges; the distances between the links of the chain can be modified with different values of S-parameter.

Following the same approach employed in **Figure 1**, an FrVL is mathematically obtained by replacing the periodic sequence by a Cantor structure developed up to certain stage. Let us consider, for example, the triadic regular Cantor sequence. The construction procedure is shown in **Figure 1a**. In the first stage, $S = 1$, the segment is divided into three parts, and the middle one is removed. In the second stage, this slicing-and-removing process is repeated in each one of the remaining two segments from the first stage. This process is repeated in the following stages. In mathematical terms, the FrVL transmittance function, for a given stage S, can be expressed by replacing the following generating function of the FrZP in Eq. **(1)** [23]:

$$q(\zeta, S; N) = \prod_{i=1}^{S} \text{rect}[\zeta^2 - 0.5]\text{rect}\left\{ \text{mod}\left[\zeta^2 - 1 + \frac{1}{(2N-1)^i}, \frac{2}{(2N-1)^i}\right] \frac{(2N-1)^i}{2} \right\} \quad (5)$$

In which the transparent and opaque zones are replaced by pure phase zones differing in π for the design wavelength. In this equation, the function $\text{mod}(x, y)$ gives the remainder on division of x by y.

Typical results are shown in **Figure 2b** for a fractal vortex lens with topological charge $m = 2$ and in **Figure 2c** for an FVL with topological charge $m = 3$.
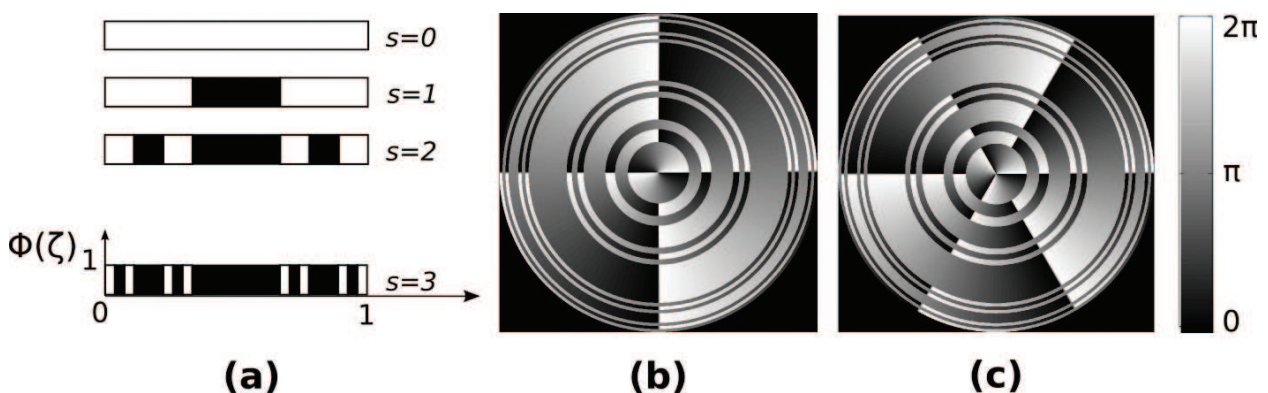

Figure 2. FVL construction: (a) Diagrams of the generation of binary function q(ζ) for an FZP for N = 2 and several values of S . (b) FVL with m=2. (c) FVL with m=3. In this representation, open and filled segments correspond to phase values differing in π of the generating radially binary function.
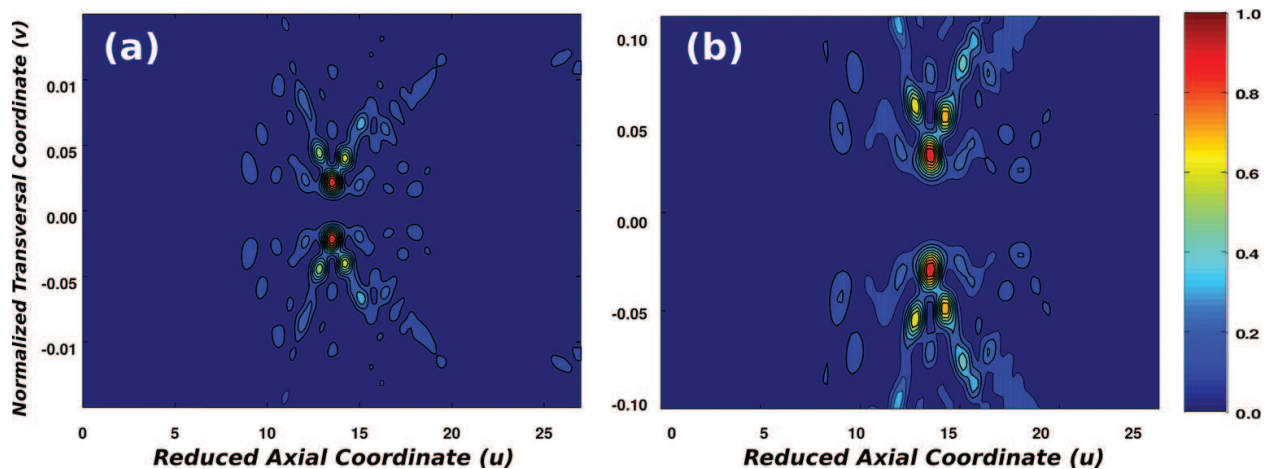
Figure 3. Normalized irradiance contours for the FVL in Figure 1: (a) $m = 2$ and (b) $m = 3$.

By using expression (4), we have computed the irradiance provided by these FrVLs at transverse planes along the optical axis. The result is shown in **Figure 3**.

As we mentioned, the diffraction efficiency of these FVLs can be improved by imposing a blazed profile to the radial coordinate. This can be done by using the Cantor function, or devil's staircase, as a generating $q(\zeta)$ function [32, 34]. The focusing properties of these FVL were experimentally analysed in [35]. It has been demonstrated that for multiple-plane optical trappings, they can generate a light beam with axially distributed optical vortices. The transverse patterns appearing along the propagation distance present several concatenated doughnut modes as represented in **Figure 3**.

Besides, the generation of multiple vortex distributions is of interest as demonstrated by the new methods that have been recently proposed to generate different two-dimensional (2D) and three-dimensional (3D) arrays of vortices. Different methods have been employed, such as interferometric techniques using Michelson or Mach-Zehnder interferometers [36] and Dammann gratings [37]. A simple method to obtain special arrays of vortices is possible by means of a reconfigurable spatial light modulator (SLM). In fact, the use of an SLM allowed the possibility to change in a simple way the characteristics of diffractive lenses, such as their focal length or their topological charge. The implementation of compound 3D optical vortex structures by means of an array of DVLs was reported in [38] with numerical simulations and experimental results.

4. Fibonacci vortex lenses

Fibonacci vortex lenses (FiVLs) are constructed using the Fibonacci sequence [22]. This sequence has been also employed in the development of different photonic devices and applications [39], such as multilayers and gratings [40], cryptography [41] and photonic crystals [42].
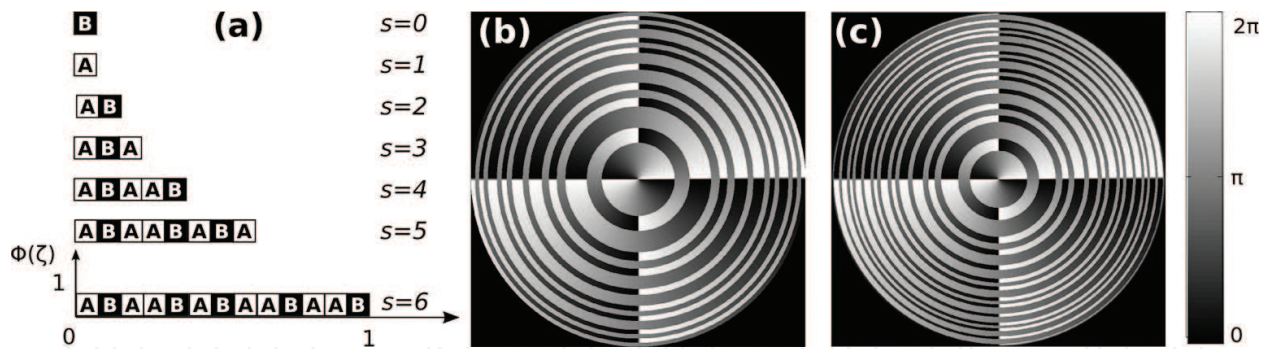
Figure 4. FiVL construction: (a) Diagrams of the generation of binary function $q(\zeta)$ for an FiZP and several values of S. (b) FiVL with $S = 7$ and $m = 2$. (c) FiVL with $S = 8$ and $m = 2$. In this representation, open and filled segments correspond to phase values differing in π of the generating radially binary function.

The Fibonacci sequence is a set of ordered numbers, $F_j = \{0, 1, 1, 2, 3, 5, 8, 13, 21,...\}$, that are obtained following a simple rule: Starting with two elements (called seeds) $F_0 = 0$ and $F_1 = 1$, the following numbers of the sequence are obtained as $F_j + 1 = F_j + F_{j-1}, (j = 0, 1, 2,...)$. The ratio of two consecutive elements of the Fibonacci sequence approaches asymptotically an irrational number known as the golden mean: $\varphi = \lim j \to \infty F_j/F_{j-1} = (1 + \sqrt{5})/2$. Fibonacci series and the golden mean have been ubiquitously observed in nature and on different scientific areas [43, 44].

Based on the Fibonacci numbers, a binary Fibonacci sequence can also be generated with two seed elements, $S_1 = \{A\}$ and $S_0 = \{B\}$, as shown in **Figure 4a**. Then, the next order of sequence is obtained simply as the concatenation of the two previous ones: $S_{j+1} = \{S_j S_{j-1}\}$ for $j \geq 1$. Consequently, $S_2 = \{AB\}, S_3 = \{ABA\}, S_4 = \{ABAAB\}, S_5 = \{ABAABABA\}$, and so on. It should be noted that the total number of elements of the order j sequence is F_{j+1} and that, for each S, two consecutive 'B' are separated by either one or two 'A'. Each sequence can be used to define the binary generating function for the radial phase distribution of the FiVL.

In our case, the function, $\Phi_j(\zeta)$, is defined in the domain $[0, 1]$, which is partitioned in F_{j+1} sub-intervals of length $d = 1/F_{j+1}$. Therefore, the function $\Phi_j(\zeta)$ at the k_{th} sub-interval is either 0 or π if the value of the k_{th} element of the S_j sequence, S_{jk}, is 'A' or 'B', respectively. Finally, after performing the coordinate transformation, $\zeta = \left(\frac{r}{a}\right)^2$, the radial part of the transmittance is obtained as $q(\zeta) = \exp[i\Phi_j(\zeta)]$ as shown in **Figure 1**.

An FiVL is defined as a pure phase diffractive element whose phase distribution is given by $\Phi_{FVL}(\zeta, \theta_0) = \mathrm{mod}2\pi[\Phi_j(\zeta) + m\theta_0]$. Thus, it combines the azimuthal phase variation that characterizes a vortex lens, with the radial phase distribution that is generated through the Fibonacci sequence. **Figure 4b** and **c** shows the results for $S = 7$ and $S = 8$ for the topological charge $m = 2$.

Compared with a Fresnel zone plates (which, we recall, can be considered periodic structures along the square radial coordinate ζ), it can be verified that if both have the same
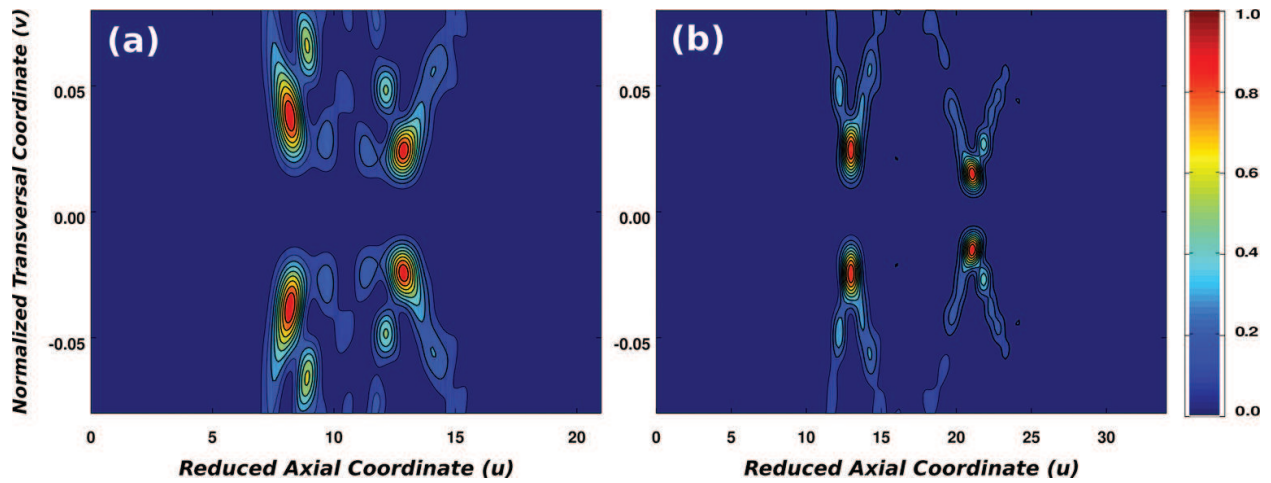
Figure 5. Normalized irradiance contours for the FVL in Figure 4: (a) FiVL $S = 7$ with $m = 2$. (b) FiVL with $S = 8, m = 2$.

number of elements, Fj, but the position of some zones with different phase has been interchanged, the FiZP produces a focal splitting of the main focus of the Fresnel zone plate along the axis. Thus, an FVL with $m = 0$ can be understood as two Fresnel zone plates interlaced [45].

The irradiances provided by the lenses are shown in **Figure 4**. The result is shown in **Figure 5**. The integrals were computed using Eq. (**4**) applying Simpson's rule with a step length 1/2000. Note that FiVLs produce twin foci whose locations are coincident with the Fibonacci numbers. In fact, for S_8 FVLs, the first focus is located at $u_1 = 13 = F_{j-1}$ and the other one at $u_2 = 21 = F_j$. Moreover, the ratio of the focal distances satisfies $\frac{u2}{u1} \approx \varphi$. The diameter of these 'twin' vortices provided by FiVLs is related by the golden mean [46], and the diameter of the rings increases proportionally with the topological charge.

5. Thue-Morse vortex lens

The Thue-Morse sequence [22] is also a binary sequence in which each element is obtained with the previous one by appending to it its Boolean complement. This sequence has been applied in several branches of Physics, as, for example, in the context of photonic crystals [47], quantum wells [48], metamaterials [49] and graphene superlattices [50].

The characteristic function q(ζ) corresponding to the Thue-Morse sequence is constructed defining a seed $D_0 = A$ from which the following elements in the sequence are obtained by replacing A by AB and B by BA. In this way, $D_1 = AB$, $D_2 = ABB$, $D_3 = BBABAAB$, $D4 = ABBABAABBAABABBA$, and so on. **Figure 6a** shows the geometrical construction of the TM sequence up to order $S = 4$. When designing Thue-Morse vortex lens (TMVL), each D_i can be used to define the transmission function $q(\zeta)$ with compact support on the interval $\zeta \in [0, 1]$. This interval is divided in 2S sub-intervals of length $dS = 1/2S$, where the transmittance, $t_{S,j}$, of the jth sub-interval is associated to the element $D_{S,j}$, as $t_{S,j} = 1$ when $D_{S,j}$ is 'A', and
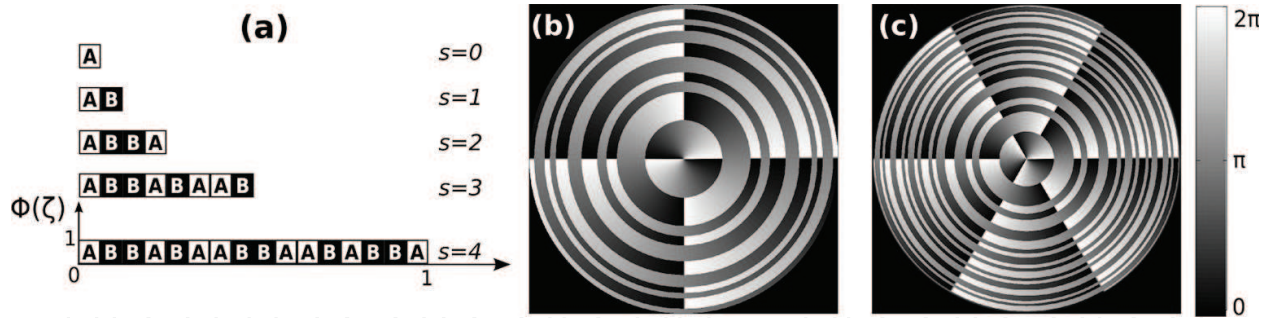
Figure 6. TMVL construction: (a) Diagrams of the generation of binary function $q(\zeta)$ for TMVL and several values of S. (b) TMVL $S = 4$ with $m = 2$. (c) TMVL $S = 5$ with $m = 3$. In this representation, open and filled segments correspond to phase values differing in $q(\zeta)$ of the generating radially binary function.
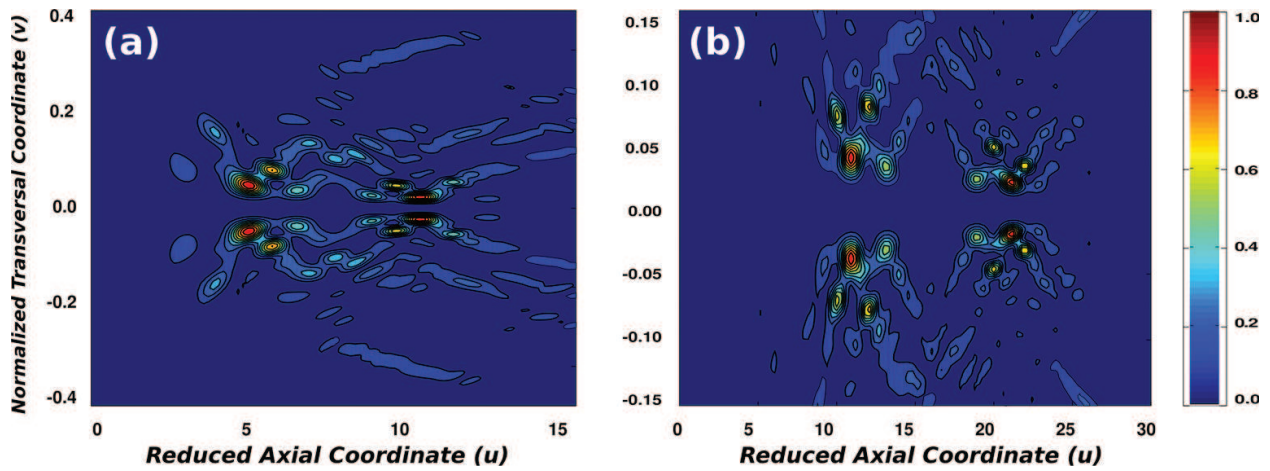

Figure 7. Normalized irradiance contours for the TMVL in Figure 7: (a) TMVL $S = 4$ with $m = 2$. (b) TMVL $S = 5$ with $m = 3$.

$t_{S,j} = 0$ when $D_{S,j}$ is $'B'$. **Figure 1**(b) shows the transmittance pupil function of a TMZP of order $S = 6$ and its equivalent periodic ZP. Note that like a conventional ZP the period of a TMZP is $pS = 2dS$, where the position of transparent/opaque zones has been interchanged. In mathematical terms, the transmittance function, $q(\zeta)$, can be written as

$$q(\zeta) = \sum_{j=1}^{2^S} t_{S,j}\text{rect}\left[\frac{\zeta-(j-0.5)d_S}{d_S}\right] \tag{6}$$

Figure 7 shows the axial irradiance provided by TMVLs of orders $S = 4$ and $S = 5$. Note that the Thue-Morse ZP produces a symmetrical splitting of the first-order focus. This zero irradiance in the middle is due to the destructive interference generated by the two conjugated parts of the lens. In this way, like FiVLs, TMVLs are bifocals, but they produce a sequence of secondary foci around each main focus that have a fractal structure. In fact, it has been shown that irradiance provided by these lenses with topological charge $m = 0$ is self-similar [51], that is, the irradiance distribution corresponding to a TMVL of order S is a

modulated version of the irradiance distribution corresponding to the previous stage, $S-1$, magnified by a factor 2.

In **Figure 7**, we represent the axial irradiances provided by the TMVLs represented in **Figure 6**. It can be seen that TMVLs produce a bifocal structure with fractal characteristic. It can also be observed that the diameters of these 'twin' vortices provided are proportional to the topological charge.

6. Experimental results

For the experimental study of the properties of FVLs, we implemented the experimental set-up shown in **Figure 8**, where the aperiodic VLs were experimentally implemented in a programmable spatial light modulator. The static aberrations caused by the SLM display were characterized with a Shack-Hartmann wavefront sensor, and then compensated as detailed elsewhere [35]. The vortex-lens performance was studied computing the diffraction patterns along different planes along the optical axis.

The proposed ZPs were recorded on a spatial light modulator (Holoeye PLUTO, eight-bit grey level, pixel size 8 μm and resolution equal to 1920 × 1080 pixels), calibrated for a 2π phase shift at $\lambda = 633$ nm operating in phase-only modulation mode. A linear phase grating was superposed to the diffractive lenses on the SLM to avoid the specular reflection and the pixelated structure of the SLM. This linear phase was compensated by an appropriate tilt of the SLM. A pin hole (PH) was used to filter high diffraction orders. A scaled image of the lens was achieved at the L3 lens focal plane (exit pupil). A collimated He-Ne laser beam ($\lambda = 633$ nm) was sent to the SLM and the diffracted field was registered with an eight-bit grey-level, charge-coupled device (CCD) camera (EO-1312M 1/2" CCD Monochrome USB Camera, pixel pitch of
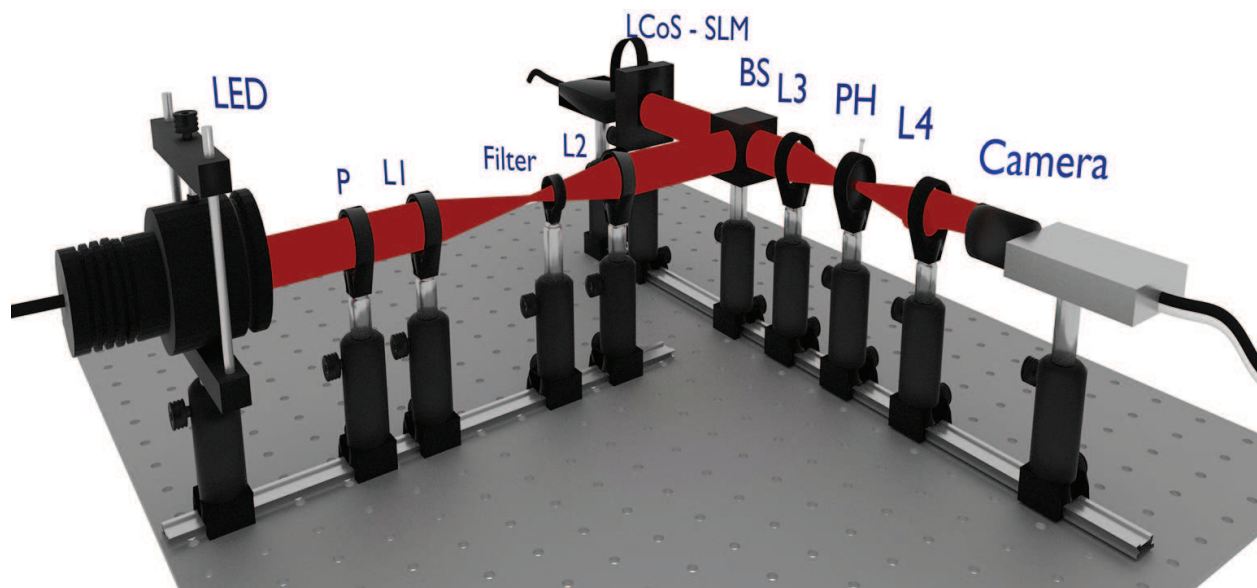

Figure 8. Experimental set-up for characterization and measuring vortices for FVLs.
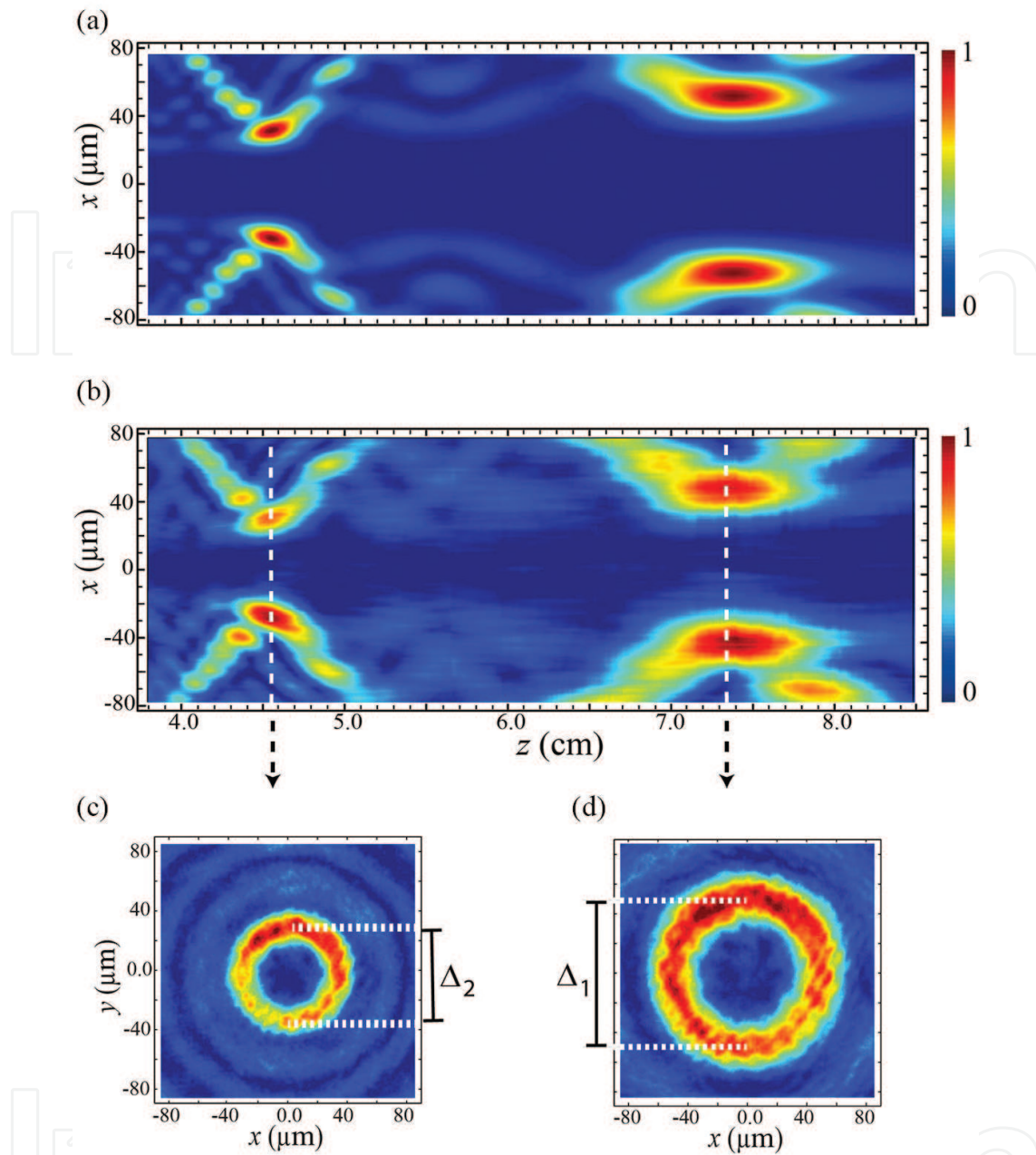
Figure 9. Longitudinal irradiance of different planes produced by $S = 8$ FiVL with $m = 6$ (a) theoretical results, (b) experimental results. (c and d) Transverse irradiance at the planes indicated by the arrows.

4.65 μm, 1280 × 1024 pixels) through a microscope objective (10× Zeiss Plan-Apochromat). The microscope and the CCD were mounted on a translation stage (Thorlabs LTS 300, range: 300 mm and 5 μm precision). The computed and experimental irradiances produced by an S8 FiVL with $m = 6$ are shown in **Figure 9**.

As predicted by the theoretical analysis (**Figure 9a**), the axial localization of the focal rings depends on the Fibonacci numbers F_j and F_{j-1}, and such focal distances satisfy the following relationship: $\frac{f1}{f2} = \frac{F_j}{F_{j-1}} \approx \Phi$. The diameter of the rings also satisfies $\frac{\Delta_1}{\Delta_2} \approx \Phi$.

7. Conclusions

A new family of fractal aperiodic VLs with interesting focusing and imaging capabilities has been presented. The transverse patterns appearing along the propagation distance present several concatenated doughnut modes. The ability of these VLs to produce multiple vortex tweezers has been demonstrated. In fact, it was found that contrary to conventional spiral zone plate, which produces a single vortex, each member of this family generates a delimited chain of vortices that are axially distributed. The distances between the links of the chain depend on the level S of the generating function and the radii of the doughnuts increase with the topological charge. Additionally, the multifocal nature of the lens, resulting from its fractal structure along the radial coordinate, could provide a high depth of field, especially with wideband sources.

In the case of FrVL (i.e. Cantor and Devil's VLs), the evolution of the axial irradiance replicates the fractality of the pupil. The orbital angular momentum in each link on the chain also depends on the topological charge but it is nearly independent of its axial location.

Our analysis demonstrated the possibility of simple design procedure arrays of VLs with any desired range of topological charge. As each individual VL can be understood as a light gear capable of driving microstructures around its circumference, applications involving particle transfer and manipulation could be foreseen.

On the other hand, FiVLs and TMVLs are intrinsically bifocal vortex lenses. It was shown that they produce twin optical vortices along the axial coordinate. The positions of both foci depend on the two incommensurable periods of the Fibonacci sequence in which the lenses are based. Moreover, the evolution of the irradiance along the propagation axis reproduces the fractality of the lens [34]. The diameter of these chains of vortices is proportional to the topological charge, and their ratio is close to the golden mean. The volumetric distribution of the diffracted field generated by FiVLs was assessed experimentally using an SLM. An excellent agreement was found between the experimental results and the theoretical predictions.

The peculiar focal volume obtained with DVLs could be exploited as versatile and efficient optical tweezer, because it can also trap low-index particles in the zero-intensity axial zone of the doughnut and at the same time can exert a torque on small objects having a high refraction index. The distances between the links of the vortex chain can be modified with the level S of the generating function and relative angular velocity of the particles at the trap depends on the topological charge of the vortex.

Another potential application of these optical vortices arises in X-ray microscopy where its azimuthal component can be used for detecting the phase component of objects with complex index of refraction since it acts as a Hilbert phase filter. This feature is especially useful in the case of biological specimens to provide enhanced contrast.

TMVL produces a couple of self-similar vortex located symmetrically one at each side of the focus of the equivalent periodic VL. Therefore, under broadband illumination, a TMVL produces a pair of images with an extended depth of field and a strong reduction in the chromatic

aberration. In this way, TMVLs combine the characteristics of FrVLs and FiVLs and could be used in multiple applications including spectral domain optical coherence tomography (OCT) and X-ray microscopy [35].

Finally, it should be mentioned that all the aperiodic VLs here presented admit fractional topological charges that break down the symmetry of the foci and produce chains of aniso-tropic vortex foci.

Acknowledgements

Author details

Federico J. Machado[1], Juan A. Monsoriu[1] and Walter D. Furlan[2]*

*Address all correspondence to: walter.furlan@uv.es

1 Centre for Physics Technologies, Polytechnic University of Valencia, Valencia, Spain

2 Department of Optics and Optometry and Vision Sciences, University of Valencia, Burjassot, Spain

References

[1] Desyatnikov A, Kivshar Y, Torner L. Optical vortices and vortex solitons. Progress in Optics. 2005;**47**:291–391. DOI: 10.1016/S0079-6638(05)47006-7

[2] Roux FS. Distribution of angular momentum and vortex morphology in optical beams. Optical Communications. 2004;**242**(1-3):45–55. DOI: 10.1016/j.optcom.2004.08.006

[3] Grier DG. A revolution in optical manipulation. Nature. 2003;**424**:810–816. DOI: 10.1038/nature01935

[4] Allen L, Padgett MJ, Babiker M. The orbital angular momentum of light. Progress in Optics. 1999;**39**:291–372. DOI: 10.1016/S0079-6638(08)70391-3

[5] Bekshaev A, Soskin M, Vasnetsov M. Paraxial Light Beams with Angular Momentum. New York, NY: Nova Publishers, 2008. arXiv:0801.2309

[6]   Lee JH, Foo G, Johnson EG, Swartzlander GA. Experimental verification of an optical vortex coronagraph. Physics Review Letters. 2006; 97. DOI: 10.1103/PhysRevLett.97.053901

[7]   Swartzlander GA Jr, Ford EL, Abdul-Malik RS, Close LM, Peters MA. Astronomical demonstration of an optical vortex coronagraph. Optical Express. 2008;**16**:10200–10207. DOI: 10.1364/OE.16.010200

[8]   Gibson G, Courtial J, Padgett M, Vasnetsov M, Pasco V. Free-space information transfer using light beams carrying orbital angular momentum. Optical Express. 2004;**12**:5448. 10.1364/OPEX.12.005448

[9]   Bouchal Z, Čelechovský R. Mixed vortex states of light as information carriers. New Journal of Physics. 2004;**6**:131. DOI:10.1088/1367-2630/6/1/131

[10] Spektor B, Normatov A, Shamir J. Singular beam microscopy. Applied Optics. 2008;**47**: A78–A87. DOI: 10.1364/AO.47.000A78

[11] Turitsyn SK, Mezentsev VK, Dubov M, Rubenchik AM, Fedoruk MP. Sub-critical regime of femtosecond inscription. Optical Express. 2007;**15**:14750–14764. DOI: 10.1364/OE.15. 014750

[12] Gahagan KT, Swartzlander GA. Optical vortex trapping of particles. Optics Letter. 1996;**21**:827–829. DOI: 10.1364/OL.21.000827

[13] Garcés-Chávez V, Volke-Sepulveda K, Chávez-Cerda S, Sibbett W, Dholakia K. Transfer of orbital angular momentum to an optically trapped low-index particle. Physics Review A. 2002;**66**:063402. DOI: 10.1103/PhysRevA.66.063402

[14] Reicherter M, Haist T, Wagemann E, Tiziani H. Optical particle trapping with computer-generated holograms written on a liquid-crystal display. Optical Letters. 1999;**24**:608–610. DOI: 10.1364/OL.24.000608

[15] Ladavac K, Grier D. Micromechanical pump assembled and driven by holographic optical vortices. Optical Express. 2004;**12**:1144–1149. DOI: 10.1364/OPEX.12.001144

[16] Friese M, Rubinsztein-Dunlop H, Gold J, Hagberg P, Hanstorp D. Optically driven micromachine elements. Applied Physics Letters. 2001;**78**:547–549. DOI: 10.1063/1.1339995

[17] Masajada J, Dubik B. Optical vortex generation by three plane wave interference. Optics Communications. 2001;**198(1)**:21–27. DOI: 10.1016/S0030-4018(01)01499-7

[18] Yang Y, Wang W, Moitra P, Kravchenko I, Briggs D, Valentine J. Dielectric meta-reflectarray for broadband linear polarization conversion and optical vortex generation. Nano Letters. 2014;**14(3)**:1394–1399. DOI: 10.1021/nl4044482

[19] Brasselet E, Murazawa N, Misawa H, Juodkazis S. Optical vortices from liquid crystal droplets. Physical Review Letters. 2009;**103(10)**:103903. DOI: 10.1103/PhysRevLett.103.103903

[20] Curtis Jennifer E, Brian AK, Grier DG. Dynamic holographic optical tweezers. Optics Communications. 2002;**207(1)**:169–175.DOI: 10.1016/S0030-4018(02)01524-9

[21] Ojeda-Castaneda J, Gomez-Reino C. Selected Papers on Zone Plates (SPIE Optical Engineering Press, 1996), vol. MS128, 512–518. DOI:10.1109/TMTT.1961.1125382

[22] Macia E. The role of aperiodic order in science and technology. Reports on Progress in Physics. 2006;**69**:397–441. DOI: 10.1088/0034-4885/69/2/R03

[23] Saavedra G, Furlan WD, Monsoriu JA, Fractal zone plates. Optical Letters. 2003;**28**:971–973. DOI: 10.1080/09500340500356973

[24]] Furlan WD, Saavedra G, Monsoriu JA. White-light imaging with fractal zone plates. Optical Letters. 2007;**32**:2109–2111. DOI: 10.1364/OL.32.002109

[25] Monsoriu JA, Calatayud A, Remon L, Furlan WD, Saavedra G, Andrés P. Bifocal Fibonacci diffractive lenses. IEEE Photonics Journal. 2013;**5**:3400106. DOI: 10.1109/ JPHOT.2013.2248707

[26] Ferrando V, Calatayud A, Andres P, Torroba R, Furlan WD, Monsoriu JA. Imaging properties of kinoform Fibonacci lenses. IEEE Photonics Journal. 2014;**6**: 6500106. DOI: 10.1109/JPHOT.2014.2304560

[27] Ferrando V, Giménez F, Furlan WD, Monsoriu JA. Bifractal focusing and imaging properties of Thue–Morse Zone Plates. Optics Express. 2015;**23(15)**:19846–19853. DOI: 10.1364/OE.23.019846

[28] Gimenez F, Furlan WD, Calatayud A, Monsoriu JA. Multifractal zone plates. Optical Society of America. 2010;**27**:1851–1855. DOI: 10.1364/JOSAA.27.001851

[29] Giménez F, Monsoriu JA, Furlan WD, Pons A. Fractal photon sieve. Optics Express. 2006;**14(25)**:11958–11963.DOI: 10.1364/OE.14.011958

[30] Giménez F, Furlan WD, Calatayud A, Monsoriu JA. Multifractal zone plates. OSA. 2010;**27(8)** :1851–1855. DOI: 10.1364/JOSAA.27.001851

[31] Tao SH, Yuan XC, Lin J, Burge R. Sequence of focused optical vortices generated by a spiral fractal zone plates. Applied Physics Letters. 2006;**89**: 031105. DOI: 10.1063/ 1.2226995

[32] Furlan WD, Giménez F, Calatayud A, Monsoriu JA. Devil's vortex-lenses. Optics Express. 2009;**17**:21891–21896. DOI: 10.1364/OE.17.021891

[33] Monsoriu JA, Furlan WD, Saavedra G, Giménez F. Devil's lenses. Optics Express. 2007;**15 (21)**:13858–13864. DOI: 10.1364/OE.15.013858

[34] Furlan WD, Giménez F, Calatayud A, Remon L, Monsoriu JA. Volumetric multiple optical traps produced by Devil's lenses. Journal of the European Optical Society-Rapid Publications. 2010;**5**:10037s. DOI: 10.2971/jeos.2010.10037s

[35] Calatayud A, Rodrigo JA, Remón L, Furlan WD, Cristóbal G, Monsoriu JA. Experimental generation and characterization of Devil's vortex-lenses. Applied Physics B. 2012;**106**:915–919. DOI: 10.1007/s00340-012-4913-0

[36] Vyas S, Senthikumaran P. Interferometric optical vortex array generator. Applied Optics. 2007;**46**:2893–2898. DOI: 10.1364/AO.46.002893

[37] García-Martínez P, Sánchez-López MM, Davis JA, Cottrell DM, Sand D, Moreno I. Generation of Bessel beam arrays through Dammann gratings. Applied Optics. 2012;**51**:1375–1381. DOI: 10.1364/AO.51.001375

[38] Calabuig A, Sánchez-Ruiz S, Martínez-León L, Tajahuerce E, Fernández-Alonso M, Furlan, WD, Pons-Martí, A. Generation of programmable 3D optical vortex structures through devil's vortex-lens arrays. Applied Optics. 2013;**52(23)**:5822–5829. DOI: 10.1364/AO.52.005822

[39] Maciá E. Exploiting aperiodic designs in nanophotonic devices. Reports in Progress on Physics. 2012;75:1–42. DOI: 10.1088/0034-4885/75/3/036502

[40] Sah Y, Ranganath G. Optical diffraction in some Fibonacci structures. Optics Communications. 1995;**114**:18–24. DOI: 10.1016/0030-4018(94)00600-Y

[41] Zhou Y, Panetta K, Agaian S, Chen CP. Image encryption using P-Fibonacci transform and decomposition. Optics Communications. 2012; **285(5)**:594-608. DOI: 10.1016/j.optcom.2011.11.044

[42] Lusk D, Abdulhalim I, Placido F. Omnidirectional reflection from Fibonacci quasi-periodic one-dimensional photonic crystal. Optics Communications. 2001;**198(4)**:273–279. DOI: 10.1016/S0030-4018(01)01531-0

[43] Basin SL. The Fibonacci sequence as it appears in nature. Fibonacci Quarterly. 1963;**1 (1)**:53–56.

[44] Garland TH. Fascinating Fibonaccis: Mystery and Magic in Numbers. Dale Seymour Publications. Palo Alto, CA 94303-0879, 1987. DOI: 10.1111/j.1949-8594.1990

[45] Monsoriu JA, Calatayud A, Remón L, Furlan WD, Saavedra G, Andrés P. Bifocal Fibonacci diffractive lenses. In IEEE Photonics Journal 2013. Vol. 5, No. 3, pp. 34001061–34001067. Institute of Electrical and Electronics Engineers (IEEE). DOI: 10.1109/JPHOT.2013.2248707

[46] Calatayud A, Ferrando V, Remón L, Furlan WD, Monsoriu JA. Twin axial vortices generated by Fibonacci lenses. Optics Express. 2013;**21(8)**:10234–10239. DOI: 10.1364/OE.21.010234

[47] Tsao CW, Cheng YH, Hsueh WJ. Localized modes in one-dimensional symmetric Thue-Morse quasicrystals. Optics Express. 2014;**22**:24378–24383. DOI: 10.1364/OE.22.024378

[48] Hsueh WJ, Chang CH, Lin CT. Exciton photoluminescence in resonant quasi-periodic Thue-Morse quantum wells. Optical Letters. 2014;**39**:489–492. DOI: 10.1364/OL.39.000489

[49] Monsoriu JA, Depine RA, Silvestre E. Non-Bragg band gaps in 1D metamaterial aperiodic multilayers Optics Express. 2007;**2**:07002. DOI: 10.1364/OE.14.012958

[50] Huang H, Liu D, Zhang H, Kong X. Electronic transport and shot noise in Thue-Morse sequence graphene superlattice. Applied Physics. 2013;**113**:043702 . DOI: 10.1142/S0217798 4916501815

[51] Ferrando V, Giménez F, Furlan WD, Monsoriu JA. Bifractal focusing and imaging properties of Thue–Morse Zone Plates. Optics Express. 2015;**23**(15):19846–19853. DOI: 10.1364/OE.23.019846.